Article

Development and Validation of Air-to-Water Heat Pump Model for Greenhouse Heating

Adnan Rasheed [1], Wook Ho Na [1], Jong Won Lee [2]‍, Hyeon Tae Kim [3]‍ and Hyun Woo Lee [1,4,*]

[1] Smart Agriculture Innovation Center, Kyungpook National University, Daegu 41566, Korea; adnanrasheed@knu.ac.kr (A.R.); wooks121@hanmail.net (W.H.N.)
[2] Department of Horticulture Environment System, Korea National College of Agriculture and Fisheries, 1515, Kongjwipatjwi-ro, Deokjin-gu, Jeonju-si 54874, Jeollabuk-do, Korea; leewon1@korea.kr
[3] Department of Bio-Industrial Machinery Engineering, Institute of Agricultural and Life Sciences, Gyeongsang National University, Jinju 660-701, Korea; bioani@gnu.ac.kr
[4] Department of Agricultural Engineering, Kyungpook National University, Daegu 702-701, Korea
[*] Correspondence: whlee@knu.ac.kr; Tel.: +82-53-950-5736

Abstract: This study proposes a building energy simulation (BES) model of an air-to-water heat pump (AWHP) system integrated with a multi-span greenhouse using the TRNSYS-18 program. The proposed BES model was validated using an experimental AWHP and a multi-span greenhouse installed in Kyungpook National University, Daegu, South Korea (latitude 35.53° N, longitude 128.36° E, elevation 48 m). Three AWHPs and a water storage tank were used to fulfill the heat energy requirement of the three-span greenhouse with 391.6 m^2 of floor area. The model was validated by comparing the following experimental and simulated results, namely, the internal greenhouse temperature, the heating load of the greenhouse, heat supply from the water storage tank to the greenhouse, heat pumps' output water temperature, power used by the heat pumps, coefficient of performance (COP) of the heat pump, and water storage tank temperature. The BES model's performance was evaluated by calculating the root mean square error (RMSE) and the Nash–Sutcliffe efficiency (NSE) coefficient of validation results. The overall results correlated well with the experimental and simulated results and encouraged adopting the BES model. The average calculated COP of the AWHP was 2.2 when the outside temperature was as low as −13 °C. The proposed model was designed simply, and detailed information of each step is provided to make it easy to use for engineers, researchers, and consultants.

Keywords: greenhouse energy modeling; renewable energy; energy-saving screen; greenhouse microclimate control

1. Introduction

Recently, greenhouse farming has increased rapidly in many countries, including South Korea. The primary objective of greenhouse farming is to obtain a year-round and high crop production in areas with severe climatic conditions unfavorable for crop production, where farming is possible only by maintaining the optimum greenhouse microclimate throughout the production period. Different heating and cooling systems are used to provide a favorable environment to crops inside the greenhouse. Therefore, fossil fuels are being used for heating and cooling, which not only increases production costs [1] but also causes CO_2 emissions and environmental pollution [2]. In South Korea, greenhouse heating costs have increased to 45% of the total production cost [3] because of continuous oil price increases. To reduce CO_2 emissions and cope with the continuously increasing oil price, the South Korean government has promoted the use of new and renewable energy (NRE) sources for different purposes, including in the agriculture sector. The NRE law was executed in 2004, enforcing the installation of the NRE systems [4].

Heat pumps are widely used in commercial as well as residential buildings [5], air-source heat pumps (ASHPs) are the most widespread heating source in commercial and

residential building due to the large availability of the external heat source and relatively low investment cost [6]. As in residential and commercial buildings, heat pumps are also being utilized in agricultural greenhouses worldwide. Many greenhouse growers have reported that using heat pumps instead of conventional heating or cooling systems reduces 80% of the fuel cost and 5–8% of total production cost [7]. Researchers have evaluated many configurations to use heat pumps for greenhouse heating under different environmental conditions [7–11]. Two types of heat pumps are used to provide heating and cooling for agricultural greenhouses, namely, ground-source water and air-source heat pumps. Ground-source heat pumps are more efficient than air-source heat pumps [12]. There are listed some studies, who investigated different heat pump systems for greenhouse heating. Seung et al. developed a ground-source heat pump to maintain the greenhouse internal setpoint temperature during winter and reported a 3.25 coefficient of performance (COP) of the heat pump in heating mode [13]. Kim et al. used thermal effluent from a power plant and applied it to a heat pump system to fulfil the heat energy requirement of the greenhouse. Furthermore, the performance of the proposed heat pump system was investigated by comparing the results with those of a conventional boiler [14]. Yildirim et al. conducted an experimental study to evaluate the ground-source heat pump (GSHP) system assisted with solar photovoltaic panels. The study considered the monthly and annual cooling and heating demand of the greenhouse, and economic analyses and payback period were also considered [15]. Boughanmi et al. studied the performance of a new conic helicoidal geothermal heat exchanger with GSHP for greenhouse heating. The analysis of the study focusses on the COP of the system [16]. Hassanien et al., in a recent study, investigated the performance of an evacuated tube solar collector as a solar water heater assisted by an electric heat pump for greenhouse heating. The analyses of this study considered the thermal efficiency of the system and payback period [17].

Many other studies have applied and evaluated ground-source heat pumps for agricultural greenhouse heating [12,18–21]. Because of low cost and ease of installation, the use of air-source heat pumps is increasing rapidly worldwide, and they show great potential for agricultural greenhouse heating [9]. Lu et al. [22] used the TRNSYS program to predict the AWHP system's performance for heating greenhouses in Melbourne, Australia. The study compared the cost of the system with that of a liquid petroleum gas (LPG) heating system and reported a six-year payback period and a 16% reduction in LPG consumption. Another study validated the TRNSYS model using experimentally obtained results for a high-temperature AWHP and thermal energy storage for a residential building [23]. The results correlated well, with a root mean square error (RMSE) of 4.14%. In a study, Moon et al. investigated the AWHP with 7.1 kW of heating capacity, along with the storage tank and heating pipes [24]. The study conducted an experimental investigation of just different heating treatments, including, growing part heating, space heating, and growing part and space heating with different temperature level controls to a small single-span greenhouse. In a recent study, Lim et al. [25] analyzed the heating performance of the air-to-water heat pump (AWHP) for greenhouses. The study focused on the COP and economic analysis of the system. The results showed an average COP of 4.5 and 70% heat energy cost reduction compared with the conventional air heater. There are many AWHP systems with different capacities available in the market. There are also many studies both simulated and experimentally conducted for the evaluation of AWHPs for greenhouse heating and cooling. The results showed the different COPs of the particular AWHPs under specific weather conditions. According to best of our knowledge, previously conducted studies were from specific points of view, and the use of a simulation model for AWHP for the specific purpose of greenhouse heating is lacking. The heat energy demand of the greenhouse and the performance of AWHP may differ depending on the different climatic conditions and the greenhouse construction and control [26]. Ensuring the accurate energy performance of the system is generally a difficult task for an HVAC designer. There is a need to develop a model that is capable of evaluation of a specific AWHP systems' efficiency with desired greenhouse construction design, including shape,

covering materials, screen materials, and environmental control inside the greenhouse under local weather conditions.

The TRNSYS program is an extremely flexible graphically based environment used to simulate the behavior of transient systems. It focuses on assessing the performance of thermal energy system simulations, including building energy simulation (BES), solar thermal processes, solar applications, geothermal energy, heat pump systems, ground-coupled heat transfer, airflow modeling, wind and photovoltaic (PV) systems, power plants, and energy system calibration. The University of Wisconsin's Solar Energy Lab developed TRNSYS, which has been commercially available since 1975 for simulating thermal systems. However, it has since undergone continuous development to become a hybrid simulator [27]. It is a component-based program simulating complex energy flows in buildings. TRNSYS can be easily connected to other programs for pre- and postprocessing the model. Over the last two decades, TRNSYS has been widely used in industry and research as a reliable tool for BES [28]. Moreover, for the modeling and simulation of agricultural greenhouses, the TRNSYS program shows high flexibility, as many greenhouse models have been developed and validated [1,29–34].

This study proposes a BES model of an AWHP system integrated with a multi-span greenhouse using the TRNSYS-18 program. The proposed model results for the internal greenhouse temperature, heat energy demand, storage tank temperature, and temperature supply and return from the heat pump and greenhouse, were validated using experimental data on the heating mode of the AWHP. Furthermore, the feasibility of the AWHP to fulfill the heat energy demand of the greenhouse was investigated. The proposed model considered all time-varying control factors of the greenhouse, including thermal screen control, ventilation control, internal temperature control, and temperature control on/off heat pump system. All physical factors of the greenhouse, including the design, covering, and screen materials and the specification of the heat pumps, storage tank, and water circulation pumps, were also considered. The study considered dynamic simulation of specific AWHP and multi-span greenhouse with fully controlled conditions under local weather conditions of Deagu, South Korea. The proposed BES model of the AWHP integrated with multi-span greenhouse was designed simply, and detailed information on each step is provided to make it easy to use for engineers, researchers, and consultants. Researcher can use this model for the dynamic thermal simulations of their specific greenhouse design and control requirements according to the local weather conditions. Moreover, AWHP analysis can help to find the feasible solution to increase the COP.

2. Materials and Methods

2.1. Experimental Greenhouse

The experimental greenhouse was a three-span rectangular, north–south (N–S) oriented, Venlo-roofed greenhouse, in which, the roof was covered with horticulture glass (HG, 4 mm) and the side walls were covered with polycarbonate (PC, 16 mm). The experimental greenhouse is in Kyungpook National University, Daegu, South Korea (latitude 35.53° N, longitude 128.36° E, elevation 48 m) (Figure 1). The total floor area of the experimental greenhouse was 391.2 m² with dimensions of 24 m × 16.3 m × 7.6 m. The experimental greenhouse was further divided into three equal parts to create different climatic conditions for different experiments. Each part's dimensions were 8 m × 16.3 m × 7.6 m, with a floor area of 130.4 m² each. HG 4 mm material was used in the division. Figure 2 shows the locations of the sensors and dimensions of the greenhouse. Weather data were recorded inside and outside the greenhouse from 1 January 2021 to 31 March 2021, during the heating period. The weather data recorded inside the greenhouse were air temperature, relative humidity, and solar radiation to validate the BES model. The weather data recorded outside the greenhouse were air temperature, relative humidity, solar radiation, and wind speed and direction. The ambient pressure data were obtained from the Korean Meteorological Administration (KMA). The outside weather data were obtained to use as input for the

BES model. Table 1 shows all recorded weather variables and their characteristics. Figure 3 shows the mean outside air temperature and solar radiation.

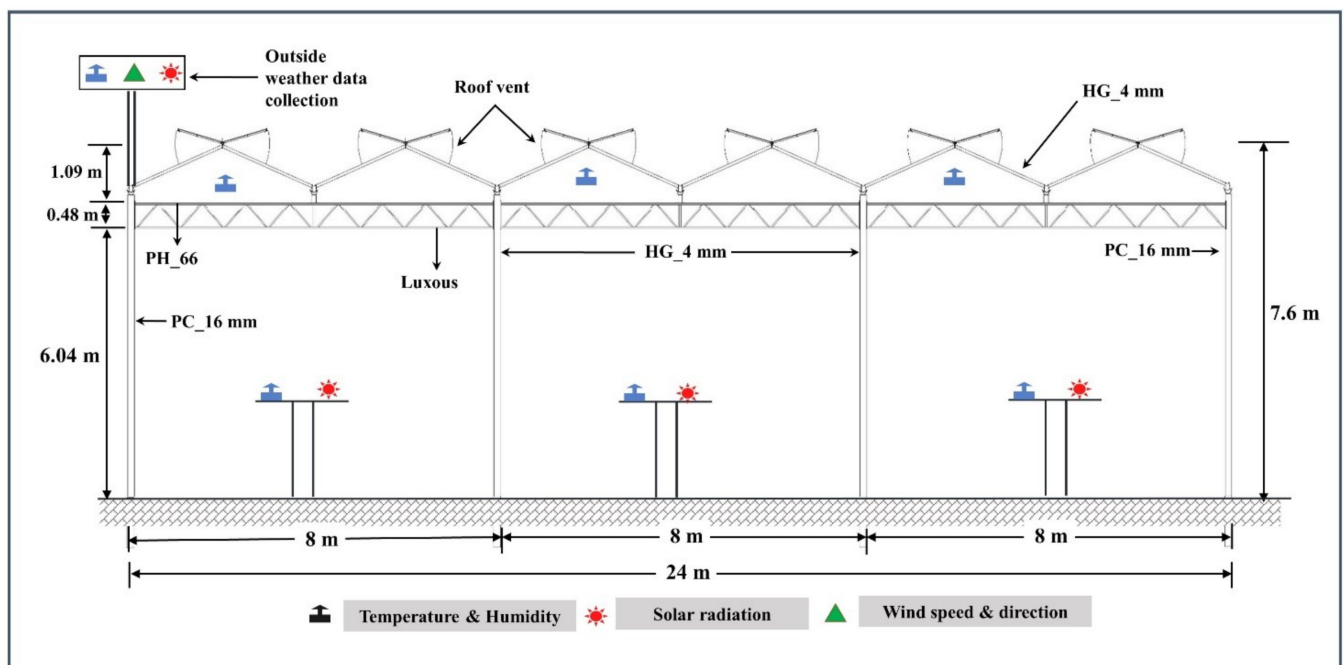**Figure 1.** Experimental greenhouse at Daegu (latitude 35.53° N, longitude 128.36° E).

Figure 2. Experimental greenhouse's dimensions and location of the sensors.

Table 1. Characteristics of the recorded weather data.

Weather Parameter	Unit	Time Interval	Sensor	Accuracy of Sensors
Air temperature	°C	10 min	MTV Active, Ridder	±1%
Relative humidity	%	10 min	MTV Active, Ridder	±2%
Solar radiation	W·m^{-2}	10 min	SR05-D2A2-TMBL, Hukseflux	IEC 61724-1:2017 standard, Class C, Basic
Wind speed	m·s^{-1}	10 min	Clima Sensor US, Thies Clima	±5%
Wind direction	degrees	10 min	Clima Sensor US, Thies Clima	±5% of measured value
Water temperature	°C	10 min	HortiMax Omni, Ridder	±0.5%
Water flow rate	Liter	10 min	FS-WLH 40, FLSTRONIC	±1% of measured value
Ambient pressure	hPa	10 min	PTB-220TS, VAISALA	±5% hPa
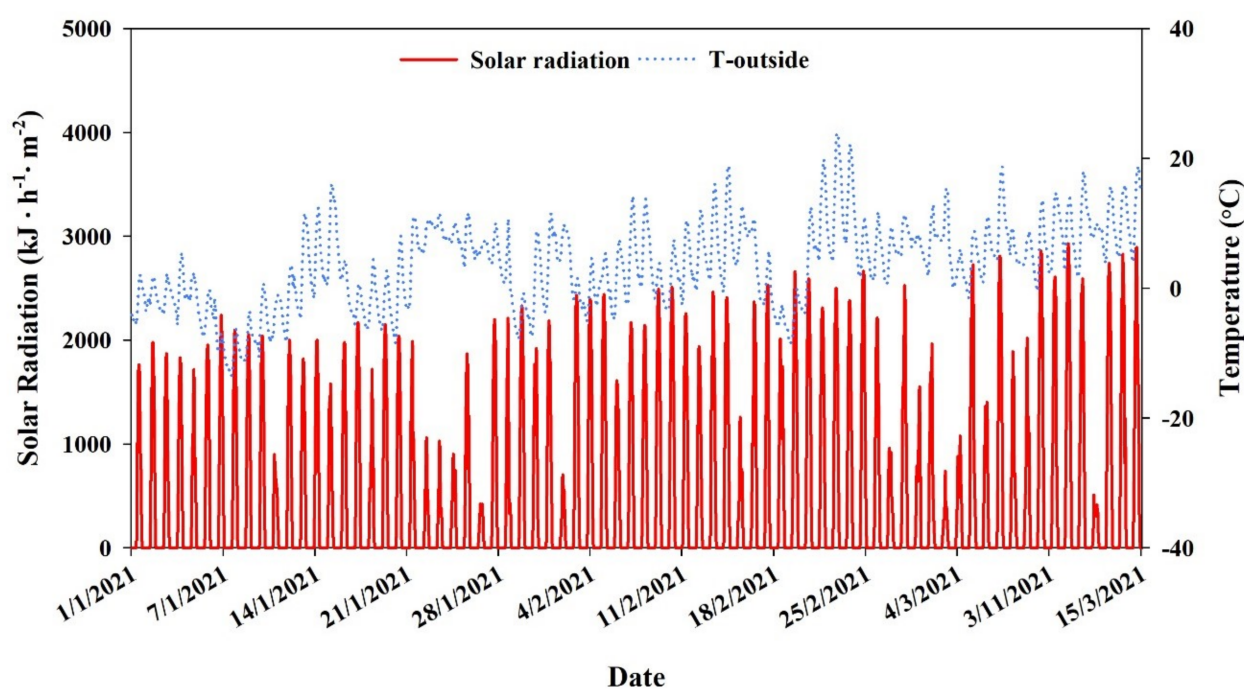
Figure 3. Ambient solar radiation and air temperature.

2.2. AWHP

Three AWHP units with a water storage tank were analyzed for their heating performance to fulfill the heat energy demand of the three-span greenhouse (detailed above). Figure 4a,b shows the experimental AWHP and the water storage tank, respectively, installed in Kyungpook National University, Daegu, South Korea. Figure 5 shows a schematic of the entire process of the AWHP in heating mode and the location of the sensors (Table 1 details the characteristics). The water storage tank stores hot water from the AWHP and supplies it to the greenhouse when heating had to reach the setpoint internal air temperature. Inside the greenhouse, heating pipes and two fan coil systems were installed to exchange heat in the greenhouse (GH3), and two fan coil systems each were used in the other two compartments (GH1 and GH2). Table 2 details the specifications of the AWHP system. We monitored the water flow rate and temperature and various locations mentioned in Figure 5 to calculate the heat energy supply from the AWHP to the water storage tank, and from the water storage tank to the greenhouse using Equation (1)

$$Q = \dot{m} \times c_p \times \Delta T \tag{1}$$

where Q is the amount of heat transfer or heating capacity of the AWHP (kJ), $\dot{m}$ is the mass flow rate (kg·s^{-1}), cp is the specific heat capacity of water (kJ·kg^{-1}·°C^{-1}), and ΔT is the temperature change (°C). Further, the COP of the heat pump was calculated using Equation (2)

$$CP = \frac{Q}{P_{HP}} \tag{2}$$

where P_{HP} is the power usage of AWHP in kJ.

Figure 4. Field picture of (**a**) AWHP and (**b**) water storage tank.
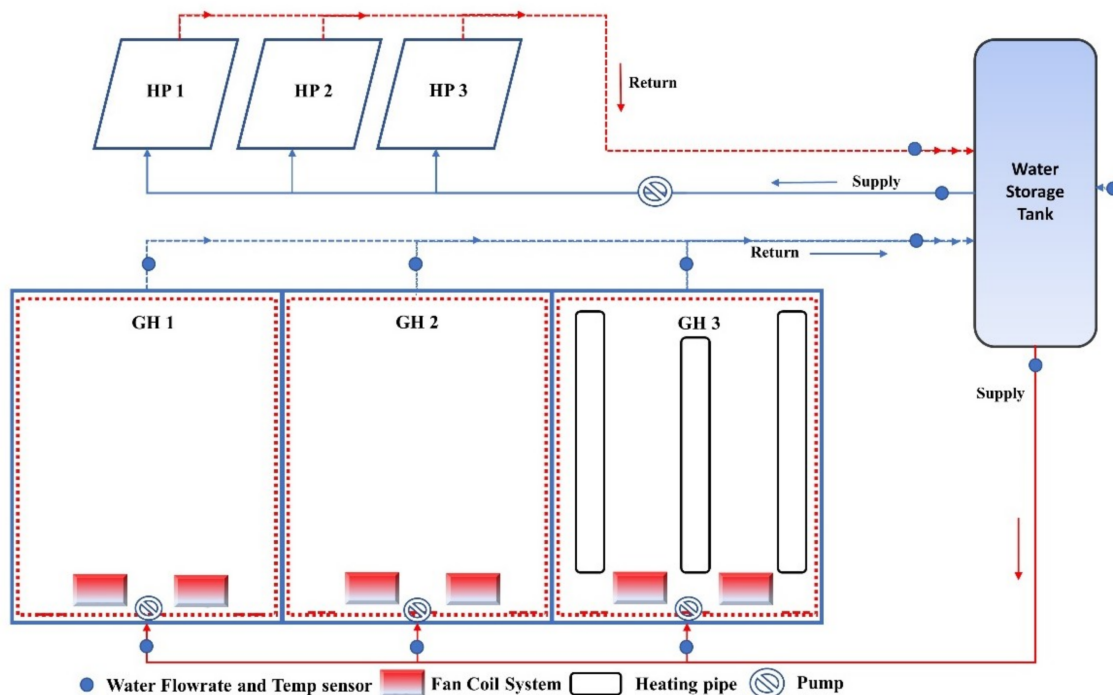

Figure 5. Schematic diagram of AWHP and location of the sensors.

Table 2. Specification of the AWHP.

Component	Properties	Specification
Heat pump	Model	PSET-C60W (MIDEA)
	Heating capacity	70 kW
	Power consumption	21.9
	Voltage	380 V–415 V, 3-phase, 60 Hz
	Refrigerant	R-410a
Heat storage tank	Heat storage fluid	Water
	Capacity	50 m^3
Water circulation pump	Model	Wilo TOP-S 40/7
	Max. fluid temperature	130 °C
	Max. fluid temperature	−20 °C
	Power consumption	390 W
Fan coil unit	Model	IN-FCG0016-L
	Heating capacity	27,000 W
	Airflow rate	83 m$^3 \cdot$m^{-1}

2.3. BES Modeling and Simulation

Designing the proposed BES model was divided into two steps. First, the greenhouse model was developed, and secondly, the heat pump system model was designed. The BES model of the AWHP system integrated, with the multi-span greenhouse with all physical and technical parameters the same as the experimental setup, was designed using the TRNSYS-18 program. Figure 6 shows the simulation studio (the main interface of the TRNSYS program) connecting all model components. Table 3 shows all components (types) and their complete descriptions, as used in the simulation studio of the TRNSYS program, to design the proposed model. First, the 3D model of the multi-span experimental greenhouse was designed in Transys3d, an add-on of Google SketchUp^{TM}, and imported as a .idf file (readable by TRNSYS) into the TRNBuild (a building interface of the TRNSYS program, TYPE 56). The greenhouse covering and screen material properties were introduced into the Lawrence Berkeley National Laboratory Windows 7.7 program, creating the DOE-2 file of the materials readable by TRNBuild. Table 4 shows the covering material and screens material's properties, while in Table 5, steel (greenhouse structure) and ground properties used in the simulation are shown. TRNBuild managed the thermal model of the building to account for natural ventilation into the greenhouse thermal model TRNSFLOW (a ventilation module of the TRNSYS program), coupling the airflow network with the thermal model to simulate the effect of natural ventilation on the greenhouse's thermal environment. Furthermore, in the simulation studio, the weather data and weather data processors were linked to the TRNBuild to simulate the effect of an ambient environment. Table 6 shows the details of the referenced greenhouse, including physical and control strategies used in the BES model simulation.

After modeling the greenhouse, the AWHP system model was prepared. Three Type 941 from the TRNSYS Tess library were used to model the AWHP. This type uses performance data files for heating and cooling provided by the manufacturer and ambient air temperature and relative humidity as input. The heating performance data file used in the simulations, and datasheet of the heat pump provided by the manufacturer can be found in Appendix A. Table 2 shows the rated heating capacity and power consumption values of the heat pump. The heat pumps are controlled with an on/off signal, as they would be in a real system. In Type 649, a water-mixing valve is used to collect hot water from all three heat pumps and deliver it to the water storage tank (Type 4). Type 114 (circulation pump) delivers cold water to the heat pump at a constant speed. From the storage tank to the fan coil unit (Type 928), hot water is provided using Type 3 (variable speed circulation pump) with a Type 22 proportional integral derivative controller to control the mass flow rate with feedback control. The fan coil unit provides hot air to the greenhouse. Moreover, Type 709 (pipe) is used inside the greenhouse to provide

heat. Hot water runs into the pipes, and heat loss from the pipes provides heat inside the greenhouse. Figure 7 shows the flow chart diagram of the proposed model, explaining the detail information of the pre-processing, simulation and output.
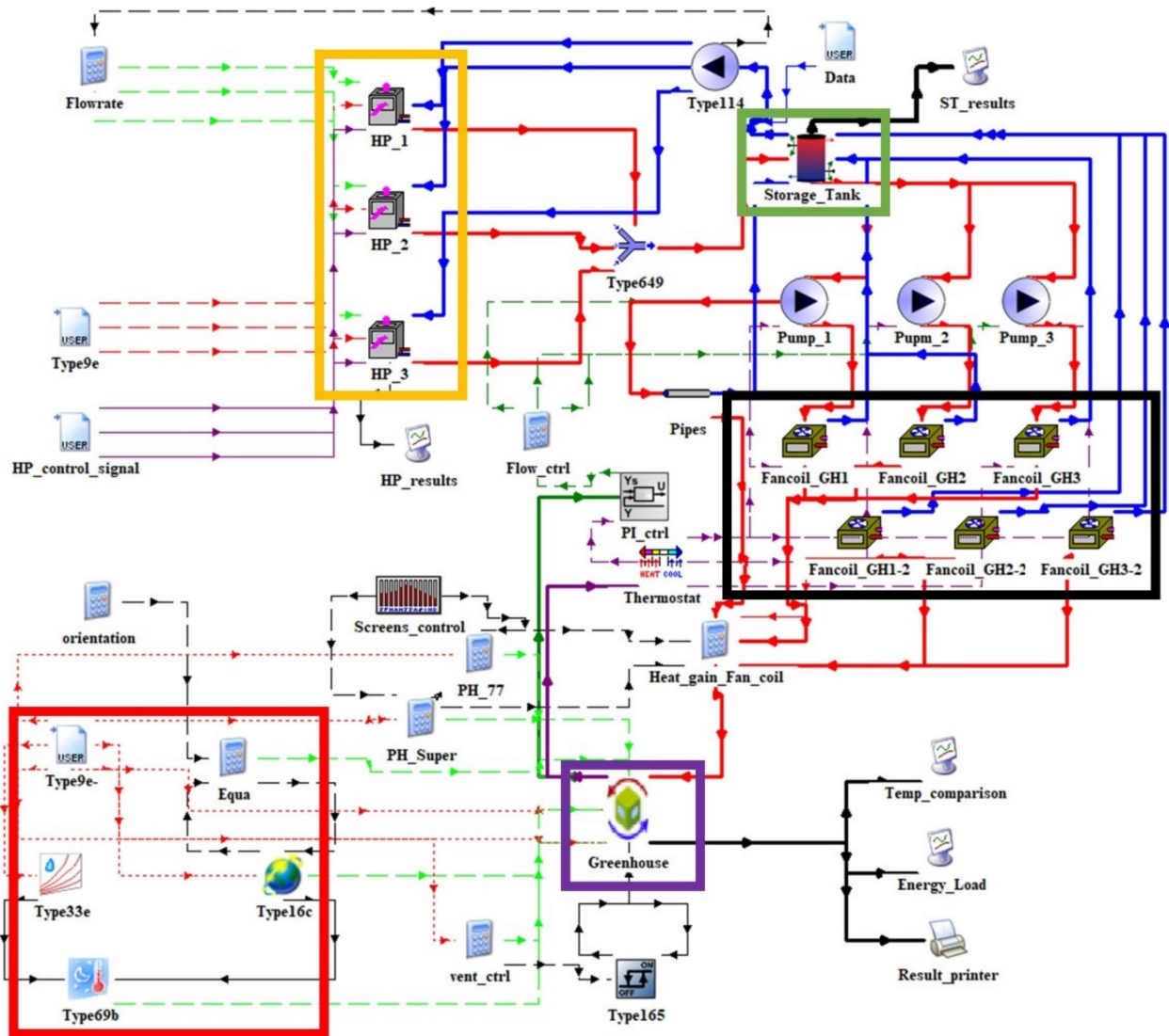

Figure 6. TRNSYS simulation studio showing proposed model's components for air-to-water heat pump system integrated with multi-span greenhouse. Yellow box: heat pump, green box: storage tank, black box: fan coil units, purple box: multi-span experimental greenhouse modeling, TRNBuild, red box: weather data reading and processing.

Table 3. Components of the greenhouse model in TRNSYS 18.

Component	Type	Description
Data reader	9	Reads the user-defined weather data file
Solar radiation processor	16	Uses total direct solar radiation on the horizontal surface as an input and calculates the total, beam, reflected, and diffuse radiation on all greenhouse tilt surfaces
Sky temperature calculator	69	Input: dewpoint temperature, beam, and diffuse radiation on horizontal surface to calculate sky temperature
Psychrometric chart	33	Calculates dewpoint temperature using dry bulk temperature and humidity ratio
Equation editor		Inserts equation in the model

Table 3. *Cont*.

Component	Type	Description
Greenhouse building model	56-TRNFlow	Uses TRNBuild and processes the thermal behavior of the greenhouse along with the natural ventilation
Air-to-water heat pump (AWHP)	941	This model is based on user-supplied data files containing catalog data for water capacity and power. It takes air-relative humidity and outside temperature as an input
Water storage tank	4	Water storage tank
Pipe	709	Models the fluid flow into the pipe; calculates the heat loss from the pipe
Fan coil unit	928	Takes hot water as an input and provides hot air to the greenhouse for temperature control
Pump	3	Variable-speed water circulation pump
Pump	114	Constant-speed water circulation pump
Valve	649	Water-mixing valve, which combines different liquid streams into a single output mass flow. Combines the output water of three heat pumps and delivers water to the storage tank
Thermostat	108	A five-stage thermostat for the on/off control function. Controls the circulation pump and fan coil unit for the greenhouse's internal temperature setpoint
Controller	165	Controls the natural ventilation of the greenhouse
Monthly forcing function	518	Inputs schedules and screen opening and closing times that change monthly
Printer	25	Prints results on user-provided external files
Plotter	65	This type was used to plot the results.

Table 4. Physical and thermal properties of the greenhouse coverings and thermal screens.

Cover Characteristics	Covering		Screens	
	HG	PC	PH_66	Luxous
Solar transmittance front	0.89	0.78	0.38	0.58
Solar transmittance back	0.89	0.78	0.38	0.57
Solar reflectance front	0.08	0.14	0.50	0.30
Solar reflectance back	0.08	0.14	0.48	0.25
Visible radiation transmittance front	0.91	0.75	0.38	0.58
Visible radiation transmittance back	0.91	0.75	0.38	0.57
Visible radiation reflectance front	0.08	0.15	0.50	0.30
Visible radiation reflectance back	0.08	0.15	0.48	0.25
Thermal radiation transmittance	0.1	0.02	0.35	0.26
Thermal radiation emission front	0.90	0.89	0.48	0.45
Thermal radiation emission back	0.90	0.89	0.55	0.42
Conductivity ($W \cdot m^{-1} \cdot K^{-1}$)	0.1	0.19	0.06	0.05
Air permeability (m^2)	—	—	1.49×10^{-11}	1.33×10^{-11}
Thickness (mm)	4	16	0.24	0.25

Table 5. Opaque materials' properties.

Material	Thickness (m)	Thermal Conductivity ($kJ \cdot h^{-1} \cdot m^{-1} \cdot K^{-1}$)	Thermal Capacity ($kJ \cdot kg^{-1} \cdot K^{-1}$)	Density ($kJ \cdot m^{-3}$)	Convective Heat Transfer Coefficient ($kJ \cdot h^{-1} \cdot m^{-2} \cdot K^{-1}$)	
					Front	Back
Steel	0.04	54	1.8	7800	11	64
Ground	0.100	0.97	0.75	2900	11	0.001

Table 6. Summary of reference three-span greenhouse.

Parameter	Operating Condition
Greenhouse type	Multi-span
Roof type	Venlo
No. of spans	3
Roof glazing	HG, 4 mm
Side glazing	PC, 16 mm
GH portion dividing glazing	HG, 4 mm
Orientation	North–South
Dimension	20.6 m × 16.3 m × 7.6 m
Floor area	391.2 m^2
Volume	2362.8 m^3
Period	1 January 2021 to 28 February 2021
Natural ventilation	roof vents
Natural vents control set point temp	26 °C
Energy screen position	Roof only
Energy screens (1 and 2)	PH-66, Luxous
Thermal screens' control	Ph-66 retract (After sunrise, OR S.R 100 W) Ph-66 Deploy (After sunset, AND S.R 100 W) Luxous_1 retract (After sunrise, OR S.R 150 W) Luxous_1 deploy (After sunset, AND S.R 150 W)
Heating setpoints, GH portion (1, 2, 3)	16, 18, and 17 °C

2.4. Statistical Analysis of BES Model

Statistical analyses were performed to predict the BES model's performance using the Nash–Sutcliffe efficiency (NSE) coefficient and compare the experimentally measured data with the BES model's output. This coefficient quantitatively describes the accuracy of the model results, it indicates how well the plot of observed versus simulated data fits the 1:1 ratio. Its value ranges from $-\infty$ to 1, and values closer to 1 indicate better predictive power of the model. The NSE is mathematically expressed using Equation (3). The performance ratings for NSE values are as follows: NSE > 0.9 = very good, 0.8–0.9 = good, 0.65–0.80 = acceptable, and <0.6 = unsatisfactory [35]. Furthermore, Equation (4) for the RMSE was used to quantify the error for units of the variables. The equations are mathematically defined as follows:

$$NSE = 1 - \left[\frac{\sum_{i=0}^{n}\left(T_i^{exp} - T_i^{sim}\right)^2}{\sum_{i=0}^{n}\left(T_i^{exp} - T_i^{mean}\right)^2} \right] \tag{3}$$

$$RMSE = \sqrt{\frac{\sum_{i=0}^{n}\left(T_i^{exp} - T_i^{sim}\right)^2}{n}} \tag{4}$$

where T_i^{exp} are the experimentally values, T_i^{sim} are the simulated values, T_i^{mean} are the mean of the experimental values, and n is the total number of observations.
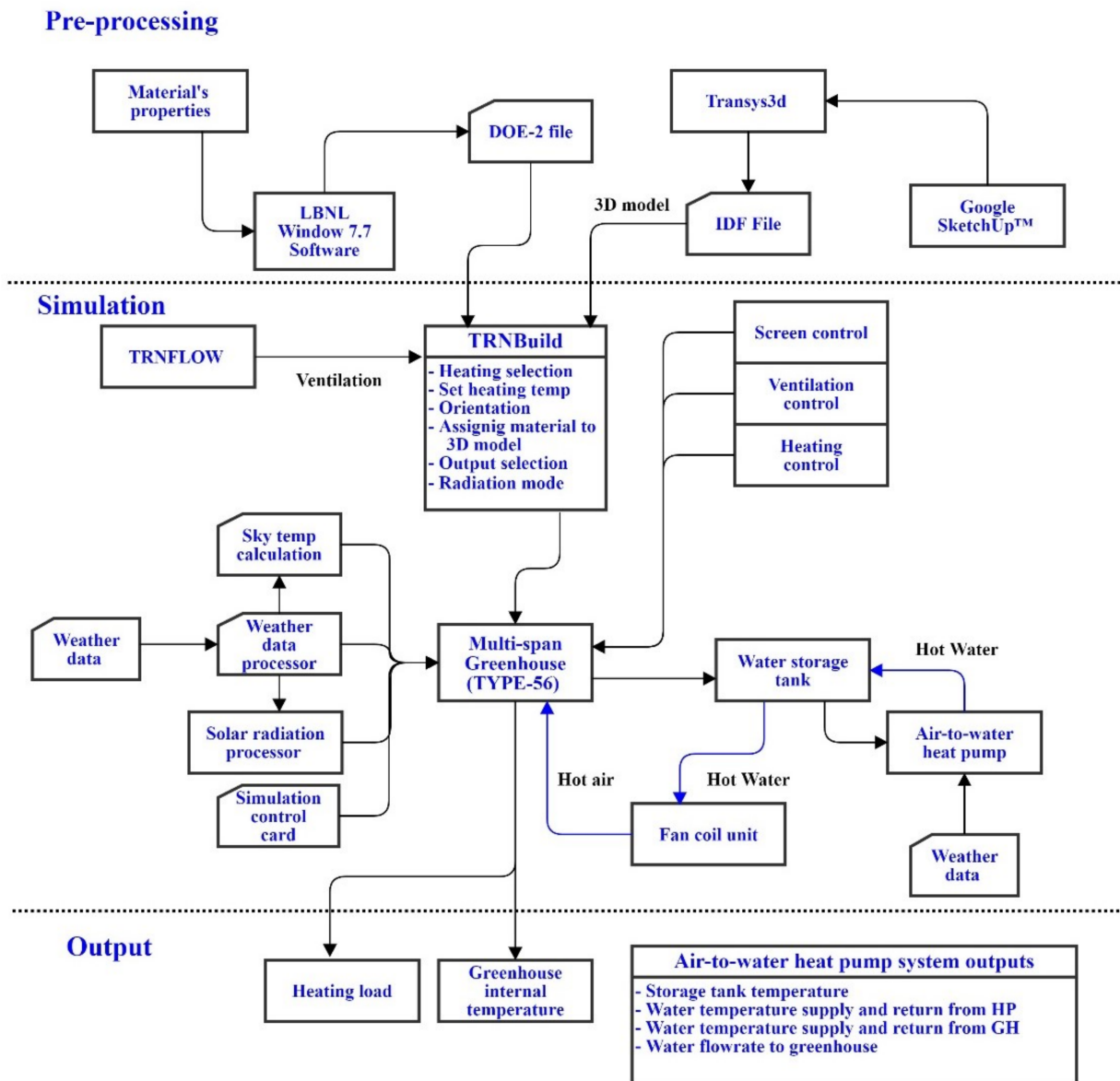
Figure 7. Flow chart of BES modeling using TRNSYS18.

3. Results and Discussion

To validate the proposed AWHP system integrated with the multi-span greenhouse BES model, the computed internal air temperature of the greenhouse, heating load, heat pump output temperature, and storage tank temperature were compared with those obtained experimentally using the same physical and operating conditions. Validation was conducted during the winter from 1 January to 31 March 2021. The normal operation of the heat pump in heating mode was repeated daily; therefore, only some days' analysis results are presented here. Figure 8 shows the greenhouse's internal experimental and simulated temperature along with the ambient temperature from 1–21 January 2021. The validation results are for all three compartments of the greenhouse, where the heating setpoint was different for each compartment. The heating setpoints were 16, 18, and 17 °C for compartments 1, 2, and 3, respectively, whereas the ventilation setpoint was 26 °C for all compartments. The simulated greenhouse internal temperature results correlated well with those of the experimentally measured temperatures. The RMSE values for the validation results were 1.9, 1.8, and 2.0 °C, indicating the maximum temperature difference between the predicted and experimental results. The NSE values were 0.71, 0.70, and 0.65, respectively, which are acceptable. Compartment 3 shows a slightly lower value because,

for some days, the experimental temperature was not well controlled to 17 °C. The overall performance analysis results show that the proposed BES model is accurate enough to predict the internal greenhouse temperature.
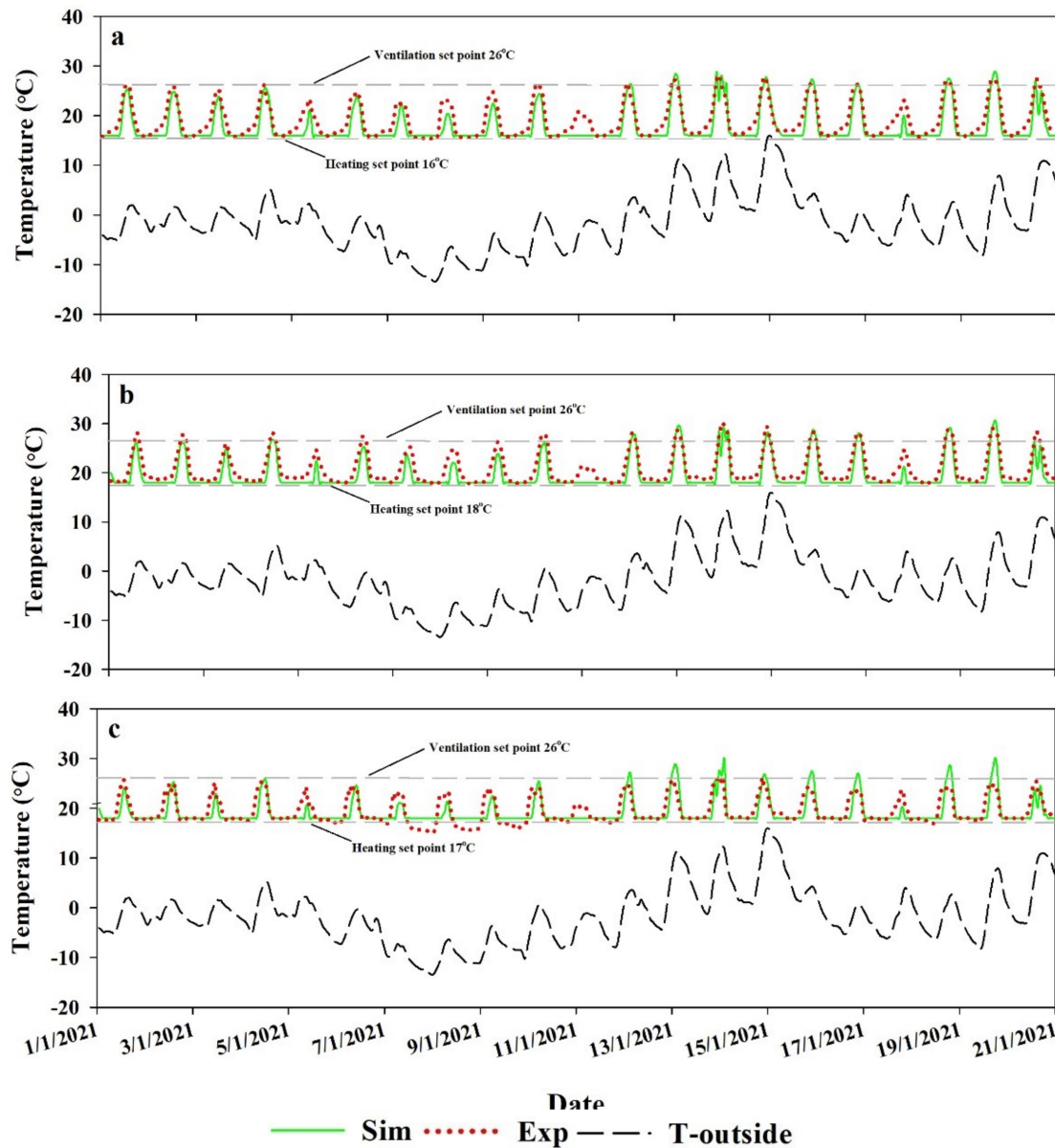

Figure 8. Experimental vs. simulated internal air temperatures (**a**) compartment 1, (**b**) compartment 2, and (**c**) compartment 3.

Figure 9a–c shows the results for experimental and simulated heating loads of all three greenhouse compartments from 1–10 January 2021, while considering the different heating setpoints for each. The maximum heating load of compartments 1, 2, and 3 were 30,000, 25,300, and 26,400 Kcal·h^{-1} on 8 January 2021, when the outside temperature was the lowest for the season (−13 °C). Figure 3 shows the ambient temperature for the entire analysis period, showing 8 January 2021, with the lowest temperature. The middle compartment showed the least heating load, even when the heating setpoint was higher than that of the other two compartments because of the reduction in heat loss. Both sidewalls were adjacent to the other compartments, and less area was exposed to the ambient environment than in the other compartments. Furthermore, compartment 3 had less heating load than that of compartment 1 because its two sidewalls were exposed to the

sun and received more solar heat during the day than compartment 1, of which only one sidewall was exposed to the sun.
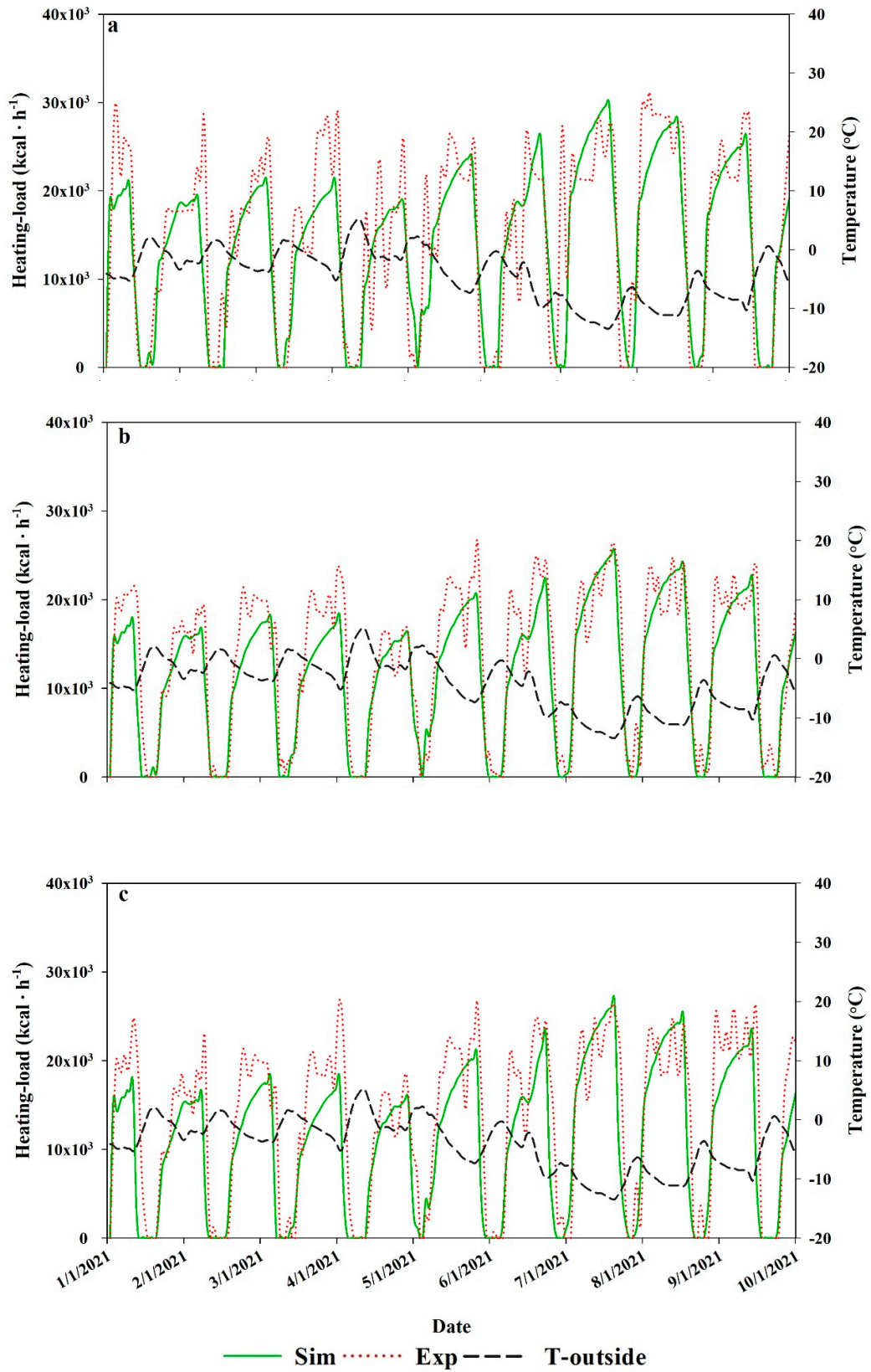

Figure 9. Experimental vs. simulated heating loads of greenhouse (**a**) compartment 1, (**b**) compartment 2, and (**c**) compartment 3.

Furthermore, the model's performance for the results shown in Figure 9 was analyzed using NSE, RMSE, and a scatter plot against a 1:1 line to visually inspect the results. Figure 10a–c shows the scatter plot for the experimental vs. simulated heating loads of the greenhouse against a 1:1 line and the NSE value. The higher performance can result in a scatter plot closer to the 1:1 line. The NSE values of 0.73, 0.81, and 0.67 for greenhouse compartments 1, 2, and 3, respectively, were acceptable. Moreover, to quantify the error for heating load units, the RMSE values of greenhouse compartments 1, 2, and 3 were 5140, 3674, and 5141 Kcal·h^{-1}. The maximum difference between the experimental and simulated results occurred on 4 January 2021, because the experimentally calculated heat load was not in a steady state, resulting in a sudden rise and fall of hot water supply to the greenhouse. Figure 9 shows that the experimentally calculated heat supply was higher on 4 January 2021, even though the outside temperature was higher than on 8 January 2021. However, the simulated results were in a steady state and showed an acceptable heating load trend with the outside temperature.
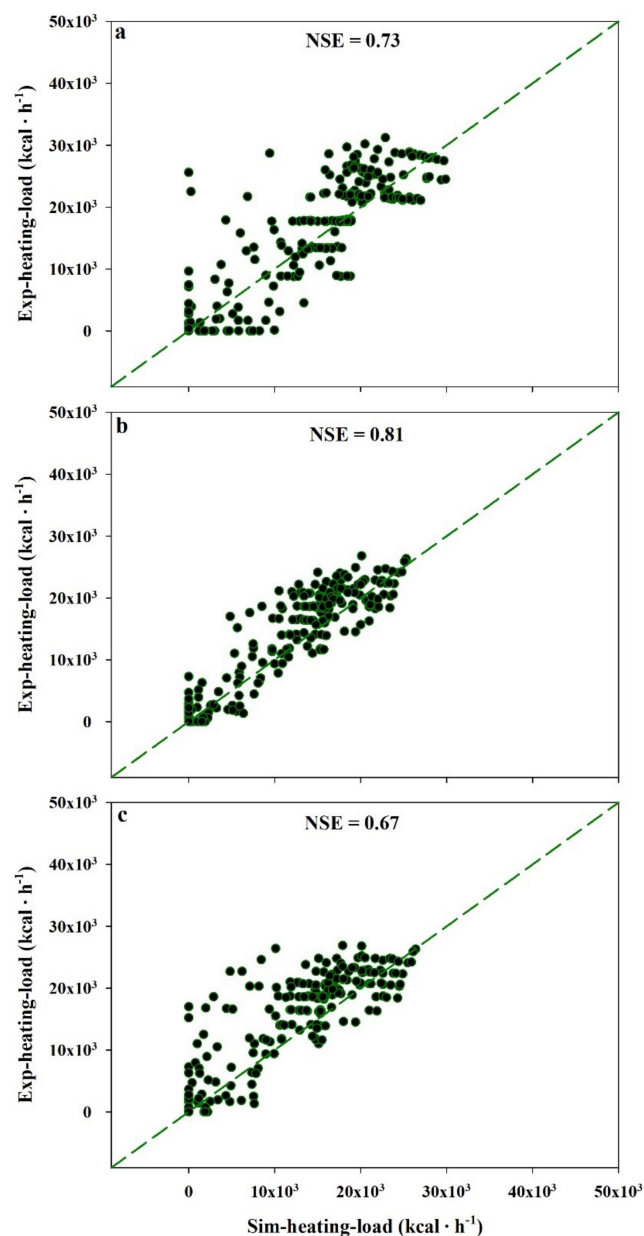

Figure 10. Statistical analysis of measured vs. computed heating loads of greenhouse (**a**) compartment 1, (**b**) compartment 2, and (**c**) compartment 3.

Figure 11 shows the results for the experimentally calculated vs. simulated heating supplied from the water storage tank to the greenhouse along with ambient air temperature from 1 January to 15 March 2021. The experimental values were calculated per unit area of the greenhouse using Equation (1) (Section 2.2) using the measured water flow rate and temperature difference between the supply and return water temperature. The results indicate that the maximum heating supplied was on 8 January 2021, as the ambient temperature was at its lowest value of $-13\ °C$. The results shown in Table 7 are the heating demand of the experimental greenhouse estimated by TRNSYS without using a particular heating system, and they confirm the maximum supplied load under the same weather conditions. The experimental results show high energy supplied to the greenhouse from 1–12 February 2021, even when the ambient temperature was high, which only occurred for one hour because of the unsteady water flow, whereas simulated results showed linear interpolated results. The overall trend and results correlated well with the validation results. Figure 12 shows that the simulated value is close enough to the experimental values, as the scattered values follow the 1:1 line. Moreover, the statistical analysis of the results shows an acceptable NSE value of 0.70 and RMSE value of 20 Kcal·h^{-1}·m^{-2}.
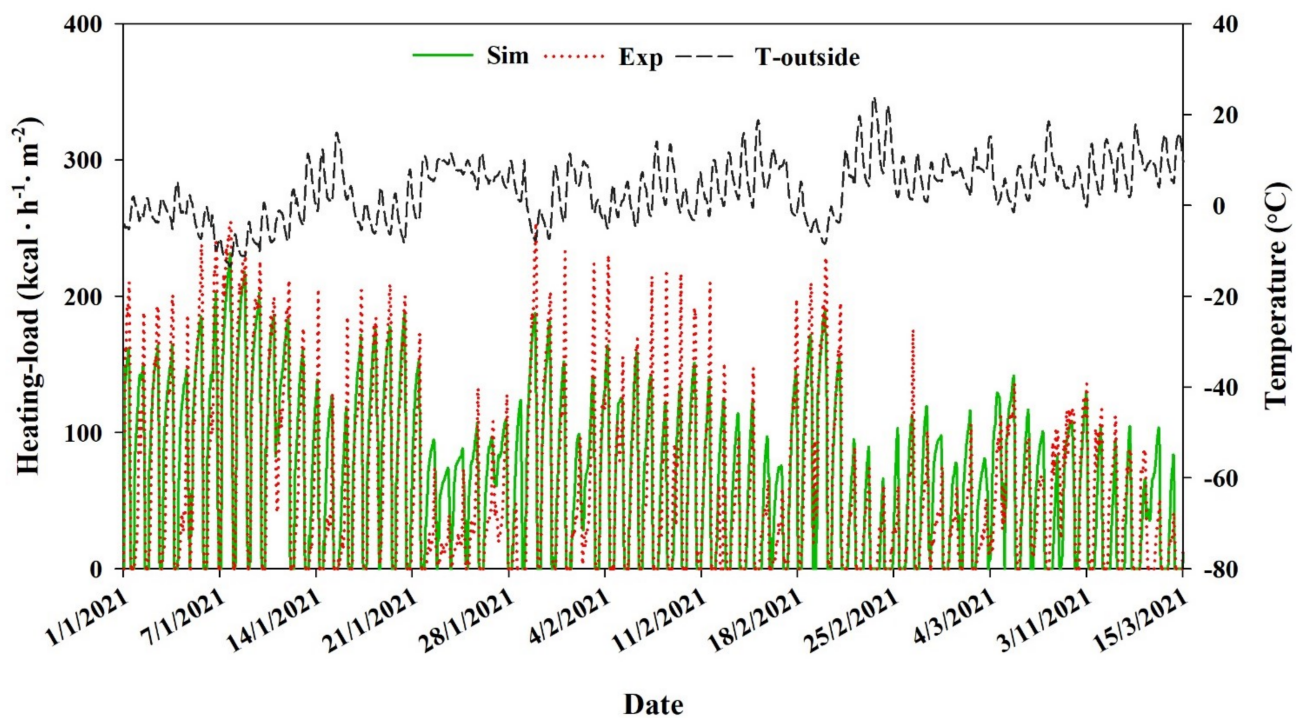

Figure 11. Experimental vs. simulated heating supply from water storage tank to greenhouse.

Table 7. TRNSYS estimated maximum heating load of the greenhouse.

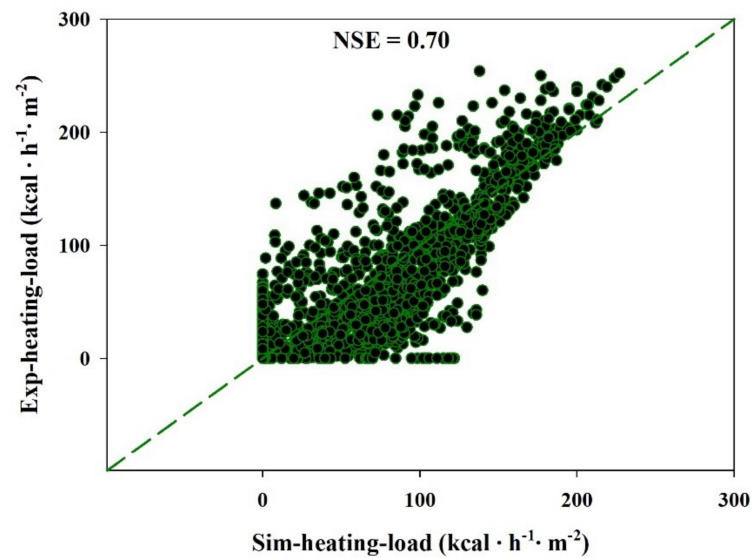| Lowest Outside Air Temp (°C)	Greenhouse Setpoint Temp (°C)	Greenhouse Heating Area (m^2)	Max. Heating Load (kcal·h^{-1})	Max. Heating Load per Unit Area (kcal·h^{-1}·m^{-2})
-13	18	391.2	97,800	250

Figure 12. Statistical analysis of measured vs. computed heating supplied from water storage tank to greenhouse.

After validating the greenhouse's internal air temperature and heating load, the experiments were further extended to validate the AWHP results. The output (hot water temperature) of the experimental heat pumps was compared with the simulated hot water temperature. Because the heat pump's function was the same throughout the season, two days' results were compared. The simulated heat pump used ambient air temperature and relative humidity as an input, and a 10 min time step, the same as the time of the data logger, was used for the simulations. The results correlated well with the experimental and simulated results (Figure 13), with a small RMSE of 0.4 °C. Three heat pumps were used in this study to heat the water and store it in the water storage tank. The storage tank temperature controlled the heat pumps' ON/OFF setting. Figure 14a–c shows the seven-day data of the experimental and simulated heat pumps, 1, 2, and 3, respectively, and the electrical consumption shows the switching ON/OFF of the heat pumps according to the need. Furthermore, the validation of both experimental and simulated results correlated well.
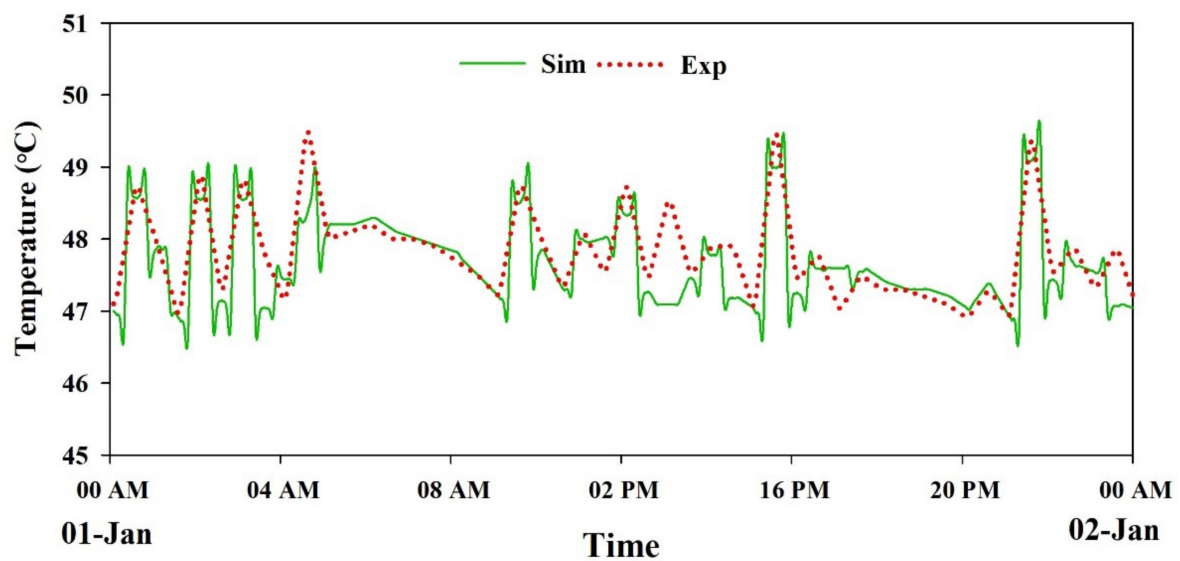

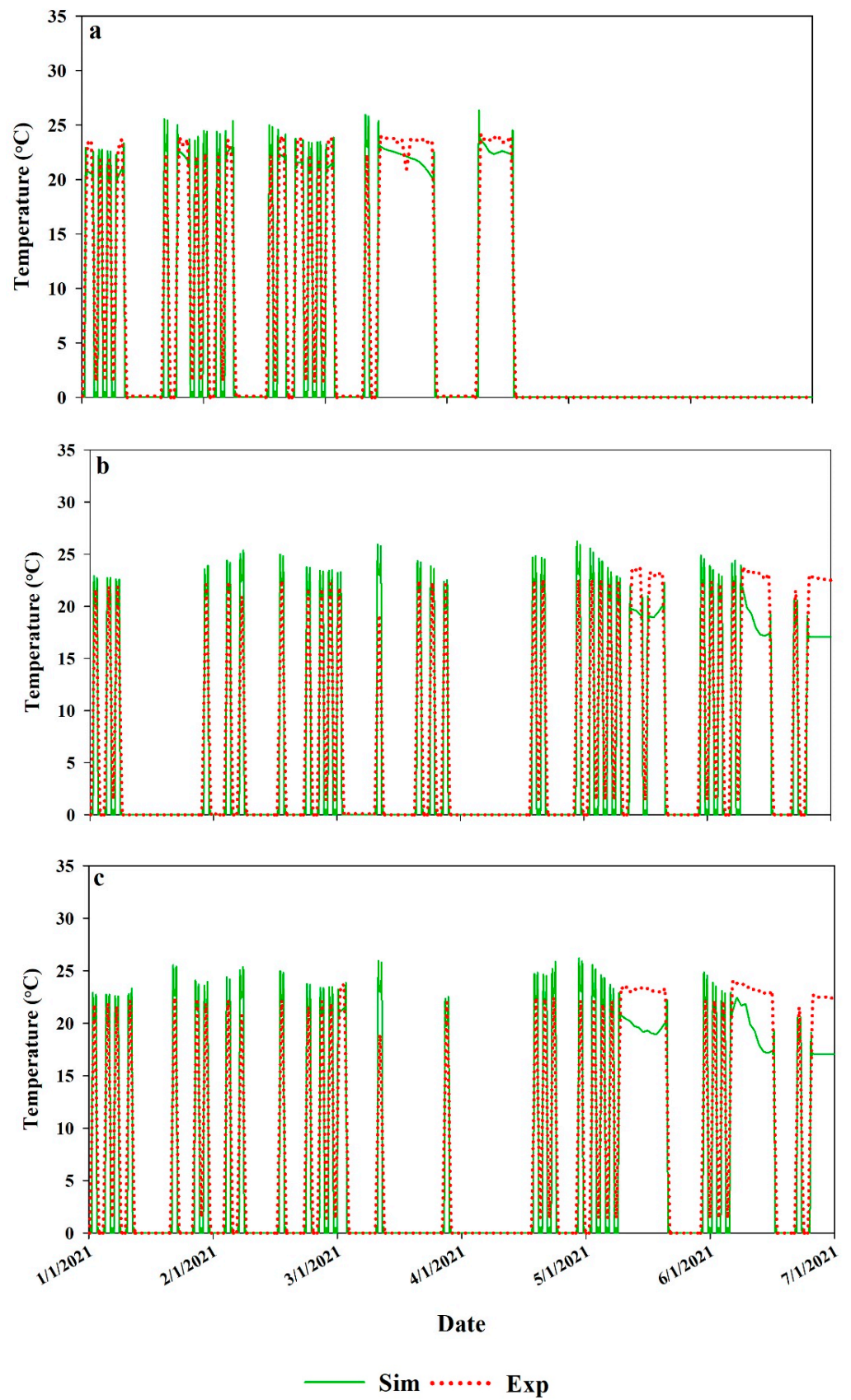**Figure 13.** Heat pump output water temperature validation.

Figure 14. Experimental and simulated power usages of (**a**) heat pump 1, (**b**) heat pump 2, and (**c**) heat pump 3.

Figure 15 shows the COP of the heat pumps with greenhouse internal and ambient temperatures. The heat pumps' heating performance was evaluated during the maximum heating requirement period. The results shown are from 7–8 January 2021, when the ambient temperature was at its lowest ($-13\,^\circ$C). The results show that when the ambient temperature starts reducing to $-13\,^\circ$C from 1 to 5 a.m., the average COP of the heat pump reduced from 2.0 to 1.7 in heating mode. The calculated average COP value of 2.2 shows the same value as the manufacturer's recommended COP for this type of AWHP.
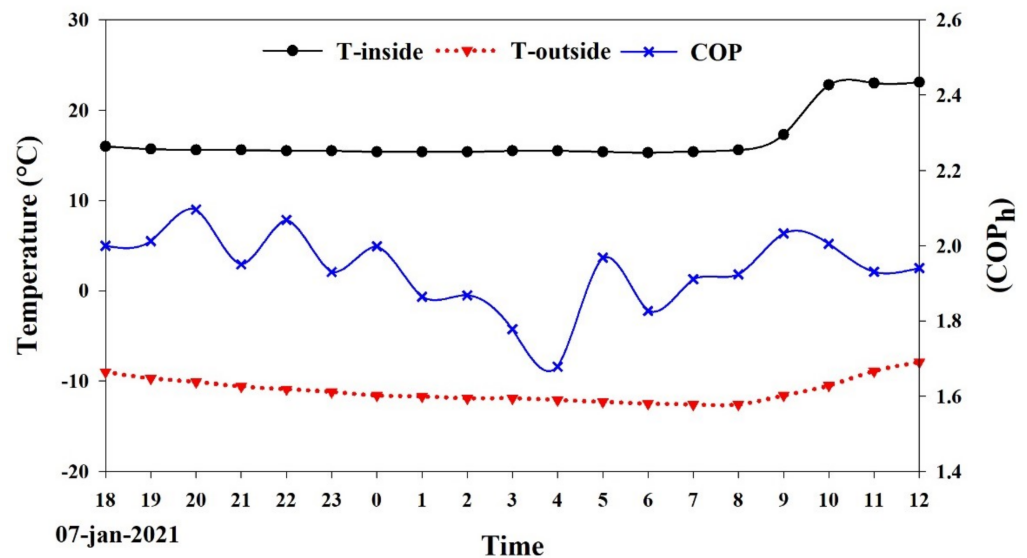

Figure 15. COP of heat pump.

Like other analyses, the normal operation of the water storage tank's charging and discharging was the same; therefore, only some days' results were shown for validation analysis (1–21 January 2021). Figure 16 shows the experimental and simulated storage tank temperatures. The validation results correlated well with an RMSE of 0.5 $^\circ$C. The validation results show that the storage tank model is fair enough to be adapted. Only one water temperature sensor was installed on the top of the tank; therefore, the average water temperature results are not shown in the study.
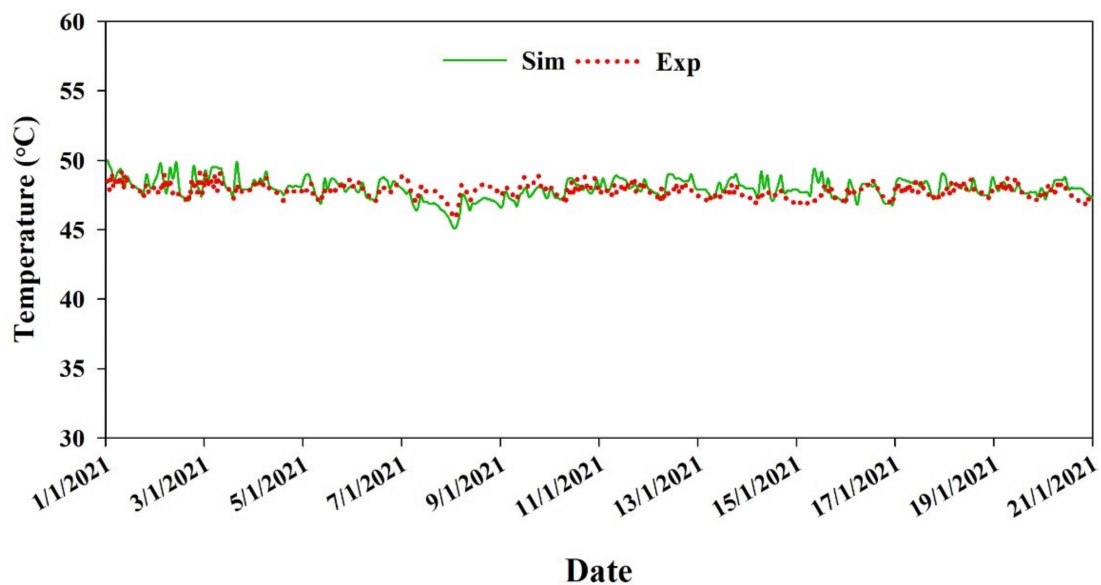

Figure 16. Water storage tank temperature validation.

4. Conclusions

This study validates the proposed BES model of an AWHP system integrated with a multi-span greenhouse using the TRNSYS-18 program. The model was validated by comparing experimental and simulated results, namely, internal air temperature of greenhouse, the heating load of the greenhouse, heat supply from the water storage tank to the greenhouse, heat pumps' output water temperature, power used by heat pumps, COP of heat pumps, and water storage tank temperature. The BES model's performance was evaluated by calculating the RMSE and NSE coefficient of validation results. The specific statistical analyses of all validation results are as follows:

- The RMSE values for the internal greenhouse air temperatures were 1.9, 1.8, and 2.0 °C, indicating the maximum temperature difference between the predicted and experimental results. The NSE values were 0.71, 0.70, and 0.65, respectively.
- The RMSE values of the energy load results for greenhouse compartments 1, 2, and 3 were 5140, 3674, and 5141 Kcal·h^{-1}, respectively, and the NSE values of greenhouse compartments 1, 2, and 3 were, 0.73, 0.81, and 0.67, respectively.
- The validation results of the energy supplied from the water storage tank to the greenhouse showed an RMSE value of 20 Kcal·h^{-1}·m^{-2} and an NSE value of 0.70.
- The heat pump output water temperature validation results showed an RMSE of 0.4 °C, and the COP of the heat pump was 2.2.
- The validation results for the water storage tank temperature show an RMSE value of 0.5 °C.
- The maximum heating energy demand for the studied greenhouse was found to be 250 kcal·h^{-1}·m^{-2}.

The overall results correlate well with experimental and simulated results and encourage adopting the BES model. The model implemented in the TRNSYS-18 program can run year-round simulations. The proposed BES model of an AWHP integrated with a multi-span greenhouse was designed simply, and detailed information on each step is provided to make it easy to use for engineers, researchers, and consultants. The presented model is developed for being used as decision-making tool for the dynamic thermal simulations of specific greenhouse design and control requirements according to the local weather conditions. All the validation results put in evidence that the proposed model is capable of evaluating such a system. Moreover, AWHP analysis can help to find a feasible solution to increase the COP. Future work will consider validating the model in the cooling mode. The proposed model can be used to optimize the control strategies and improvements to systems.

Institutional Review Board Statement: Not applicable.

Informed Consent Statement: Not applicable.

Data Availability Statement: Not applicable.

Conflicts of Interest: There is no conflict of interest regarding the publication of this research.

Appendix A

The AWHP model component in the TRNSYS requires a heating performance data file as an input. Table A1 shows the heating performance data used in the study, as provided by the manufacturer. Table A2 presents the data sheet provided by the manufacturer and the testing conditions of the heat pump.

Table A1. Heating performance data of AWHP.

25	30	35	40	45	50	T_water_in
2.2	7.2	12.2	15	20		T_air_in
0.759	0.787	!Fraction capacity and power at T_air = 2.2				deg. C and T_water_in = 25
1.08	0.868	!Fraction capacity and power at T_air = 7.2				deg. C and T_water_in = 25
1.137	0.843	!Fraction capacity and power at T_air = 12.2				deg. C and T_water_in = 25
1.233	0.843	!Fraction capacity and power at T_air = 15				deg. C and T_water_in = 25
1.403	0.844	!Fraction capacity and power at T_air = 20				deg. C and T_water_in = 25
0.737	0.86	!Fraction capacity and power at T_air = 2.2				deg. C and T_water_in = 30
1.048	0.938	!Fraction capacity and power at T_air = 7.2				deg. C and T_water_in = 30
1.106	0.923	!Fraction capacity and power at T_air = 12.2				deg. C and T_water_in = 30
1.199	0.924	!Fraction capacity and power at T_air = 15				deg. C and T_water_in = 30
1.359	0.924	!Fraction capacity and power at T_air = 20				deg. C and T_water_in = 30
0.714	0.944	!Fraction capacity and power at T_air = 2.2				deg. C and T_water_in = 35
1.017	1.044	!Fraction capacity and power at T_air = 7.2				deg. C and T_water_in = 35
1.075	1.016	!Fraction capacity and power at T_air = 12.2				deg. C and T_water_in = 35
1.165	1.017	!Fraction capacity and power at T_air = 15				deg. C and T_water_in = 35
1.314	1.018	!Fraction capacity and power at T_air = 20				deg. C and T_water_in = 35
0.692	1.027	!Fraction capacity and power at T_air = 2.2				deg. C and T_water_in = 40
0.986	1.136	!Fraction capacity and power at T_air = 7.2				deg. C and T_water_in = 40
1.043	1.108	!Fraction capacity and power at T_air = 12.2				deg. C and T_water_in = 40
1.131	1.109	!Fraction capacity and power at T_air = 15				deg. C and T_water_in = 40
1.269	1.112	!Fraction capacity and power at T_air = 20				deg. C and T_water_in = 40
0.67	1.132	!Fraction capacity and power at T_air = 2.2				deg. C and T_water_in = 45
0.955	1.255	!Fraction capacity and power at T_air = 7.2				deg. C and T_water_in = 45
1.012	1.224	!Fraction capacity and power at T_air = 12.2				deg. C and T_water_in = 45
1.097	1.226	!Fraction capacity and power at T_air = 15				deg. C and T_water_in = 45
1.224	1.229	!Fraction capacity and power at T_air = 20				deg. C and T_water_in = 45
0.648	1.249	!Fraction capacity and power at T_air = 2.2				deg. C and T_water_in = 50
0.923	1.385	!Fraction capacity and power at T_air = 7.2				deg. C and T_water_in = 50
0.981	1.352	!Fraction capacity and power at T_air = 12.2				deg. C and T_water_in = 50
1.062	1.355	!Fraction capacity and power at T_air = 15				deg. C and T_water_in = 50
1.18	1.359	!Fraction capacity and power at T_air = 20				deg. C and T_water_in = 50

Table A2. Manufacturer's data sheet of the studied AWHP.

Hot Water Outlet Temperature	Ambient Temperature °C													
	−10		−6		−2		2		7		10		13	
	Capacity	Power	Capacity	Power	Capacity	Power	Capacity	Power	Capacity	Power	Capacity	Power	Capacity	Power
°C	kW	kW	kW	kW	kW	kW	kW	kW	kW	kW	kW	kW	kW	kW
40	43.51	13.70	54.39	15.57	63.98	17.30	71.09	18.81	77.28	19.80	86.55	20.98	99.53	22.66
41	42.05	13.98	52.63	15.89	61.98	17.65	68.95	19.19	75.03	20.20	83.88	21.41	96.29	23.12
42	40.83	14.27	51.17	16.21	60.34	18.01	67.19	19.58	73.20	20.61	81.69	21.85	93.61	23.60
43	39.85	14.56	50.0	16.54	59.03	18.38	65.80	19.98	71.76	21.03	79.94	22.29	91.45	24.08
44	39.08	14.86	49.09	16.88	58.03	18.76	64.76	20.39	70.70	21.46	78.62	22.75	89.78	24.57
45	38.51	15.16	48.44	17.23	57.32	19.14	64.05	20.81	70.00	21.90	77.70	23.21	88.58	25.07
46	37.76	15.31	47.55	17.40	56.34	19.33	63.02	21.01	68.95	22.12	76.40	23.45	86.94	25.32
47	36.64	15.62	46.20	17.75	54.81	19.72	31.38	21.43	67.23	22.56	74.35	23.92	84.46	25.83
48	35.19	16.09	44.44	18.28	52.77	20.31	59.16	22.08	64.87	23.24	71.62	24.63	81.22	26.60
49	33.28	16.73	42.07	19.01	50.02	21.12	56.14	22.96	61.63	24.17	67.92	25.62	76.88	27.67
50	31.14	17.57	39.41	19.96	46.92	22.18	52.72	24.11	57.93	25.38	63.73	26.90	72.01	29.05

Capacity calculation standard for heating: inlet/outlet water temperature: 40 °C/45 °C, ambient temperature: 7 °C. Nominal data are shown with a gray background.

References

1. Rasheed, A.; Lee, J.; Lee, H. Development and optimization of a building energy simulation model to study the effect of greenhouse design parameters. *Energies* **2018**, *11*, 2001. [CrossRef]
2. Bartzanas, T.; Tchamitchian, M.; Kittas, C. Influence of the heating method on greenhouse microclimate and energy consumption. *Biosyst. Eng.* **2005**, *91*, 487–499. [CrossRef]
3. Yang, S.H.; Lee, C.G.; Lee, W.K.; Ashtiani, A.A.; Kim, J.Y.; Lee, S.D.; Rhee, J.Y. Heating and cooling system for utilization of surplus air thermal energy in greenhouse and its control logic. *J. Biosyst. Eng.* **2012**, *37*, 19–27. [CrossRef]
4. Lee, J.-Y. Current status of ground source heat pumps in korea. *J. Renew. Sustain. Energy Rev.* **2009**, *13*, 1560–1568. [CrossRef]
5. Dongellini, M.; Morini, G.L. On-off cycling losses of reversible air-to-water heat pump systems as a function of the unit power modulation capacity. *Energy Convers. Manag.* **2019**, *196*, 966–978. [CrossRef]
6. Zhang, Q.; Zhang, L.; Nie, J.; Li, Y. Techno-economic analysis of air source heat pump applied for space heating in northern china. *Appl. Energy* **2017**, *207*, 533–542. [CrossRef]
7. Carlini, M.; Monarca, D.; Biondi, P.; Honorati, T.; Castellucci, S. A simulation model for the exploitation of geothermal energy for a greenhouse in the viterbo province. In *Work Safety and Risk Prevention in Agro-Food and Forest Systems, Proceedings of the International Conference Ragusa SHWA2010, Ragusa Ibla, Italy, 16–18 September 2010*; ElleDue Editore: Ragusa Ibla, Italy, 2010; pp. 16–18.
8. Kozai, T. Thermal performance of an oil engine driven heat pump for greenhouse heating. *J. Agric. Eng. Res.* **1986**, *35*, 25–37. [CrossRef]
9. Tong, Y.; Kozai, T.; Nishioka, N.; Ohyama, K. Greenhouse heating using heat pumps with a high coefficient of performance (cop). *Biosyst. Eng.* **2010**, *106*, 405–411. [CrossRef]
10. Chargui, R.; Sammouda, H.; Farhat, A. Geothermal heat pump in heating mode: Modeling and simulation on trnsys. *Int. J. Refrig* **2012**, *35*, 1824–1832. [CrossRef]
11. Rasheed, A.; Lee, J.W.; Lee, H.W. A review of greenhouse energy management by using building energy simulation. *Prot. Hortic. Plant. Fact.* **2015**, *24*, 317–325. [CrossRef]
12. Benli, H.; Durmuş, A. Evaluation of ground-source heat pump combined latent heat storage system performance in greenhouse heating. *Energy Build.* **2009**, *41*, 220–228. [CrossRef]
13. Yang, S.-H.; Lee, S.-D.; Kim, Y.J.R. Greenhouse heating and cooling with a heat pump system using surplus air and underground water thermal energy. *Eng. Agric. Environ. Food* **2013**, *6*, 86–91. [CrossRef]
14. Kim, M.-H.; Lee, D.-W.; Yun, R.; Heo, J. Operational energy saving potential of thermal effluent source heat pump system for greenhouse heating in jeju. *Int. J. Air Cond. Refrig.* **2017**, *25*, 01–12. [CrossRef]
15. Yildirim, N.; Bilir, L. Evaluation of a hybrid system for a nearly zero energy greenhouse. *Energy Convers. Manag.* **2017**, *148*, 1278–1290. [CrossRef]
16. Boughanmi, H.; Lazaar, M.; Guizani, A. A performance of a heat pump system connected a new conic helicoidal geothermal heat exchanger for a greenhouse heating in the north of tunisia. *Sol. Energy* **2018**, *171*, 343–353. [CrossRef]
17. Hassanien, R.H.E.; Li, M.; Tang, Y. The evacuated tube solar collector assisted heat pump for heating greenhouses. *Energy Build.* **2018**, *169*, 305–318. [CrossRef]
18. Ozgener, O.; Hepbasli, A. Experimental investigation of the performance of a solar-assisted ground-source heat pump system for greenhouse heating. *Int. J. Energy Res.* **2005**, *29*, 217–231. [CrossRef]
19. Ozgener, O.; Hepbasli, A. Experimental performance analysis of a solar assisted ground-source heat pump greenhouse heating system. *Energy Build.* **2005**, *37*, 101–110. [CrossRef]
20. Ozgener, O.; Hepbasli, A. A parametrical study on the energetic and exergetic assessment of a solar-assisted vertical ground-source heat pump system used for heating a greenhouse. *Build. Environ.* **2007**, *42*, 11–24. [CrossRef]
21. Ozgener, O. Use of solar assisted geothermal heat pump and small wind turbine systems for heating agricultural and residential buildings. *J. Energy* **2010**, *35*, 262–268. [CrossRef]
22. Aye, L.; Fuller, R.J.; Canal, A. Evaluation of a heat pump system for greenhouse heating. *Int. J. Therm. Sci.* **2010**, *49*, 202–208. [CrossRef]
23. Le, K.; Shah, N.; Huang, M.; Hewitt, N. High temperature air-water heat pump and energy storage: Validation of trnsys models. In Proceedings of the World Congress on Engineering and Computer Science WCECS 2017, San Francisco, CA, USA, 25–27 October 2017; Volume II.
24. Moon, J.; Kwon, J.; Kim, S.; Kang, Y.; Park, S.; Lee, J. Effect on yield increase and energy saving in partial heating for high-bed strawberries by using an air to water heat pump. In Proceedings of the 2019 ASABE Annual International Meeting, Boston, MA, USA, 7–10 July 2019; American Society of Agricultural and Biological Engineers: Boston, MA, USA, 2019; p. 1.
25. Lim, T.; Baik, Y.-K.; Kim, D.D. Heating performance analysis of an air-to-water heat pump using underground air for greenhouse farming. *Energies* **2020**, *13*, 3863. [CrossRef]
26. Nemś, A.; Nemś, M.; Świder, K. Analysis of the possibilities of using a heat pump for greenhouse heating in polish climatic conditions—A case study. *Sustainability* **2018**, *10*, 3483. [CrossRef]
27. Klein, S.A. Trnsys, a transient system simulation program. In *Solar Energy Laboratory*; University of Wisconsin: Madison, WI, USA, 2012.

28. Casetta, D. Implementation and Validation of a Ground Source Heat Pump Model in Matlab. Master's Thesis, Chalmers University of Technology, Gothenburg, Sweden, 2012.
29. Rasheed, A.; Na, W.H.; Lee, J.W.; Kim, H.T.; Lee, H.W. Optimization of greenhouse thermal screens for maximized energy conservation. *Energies* **2019**, *12*, 3592. [CrossRef]
30. Rasheed, A.; Kwak, C.S.; Na, W.H.; Lee, J.W.; Kim, H.T.; Lee, H.W. Development of a building energy simulation model for control of multi-span greenhouse microclimate. *Energies* **2020**, *10*, 1236. [CrossRef]
31. Lee, S.-N.; Park, S.-J.; Lee, I.-B.; Ha, T.-H.; Kwon, K.-S.; Kim, R.-W.; Yeo, U.-H.; Lee, S.-Y. Design of energy model of greenhouse including plant and estimation of heating and cooling loads for a multi-span plastic-film greenhouse by building energy simulation. *Prot. Hortic. Plant. Fact.* **2016**, *25*, 123–132. [CrossRef]
32. Seo, I.-H.; Lee, I.-B.; Kwon, K.-S.; Park, S.-J.J.A.H. Bes computation for periodical energy load of greenhouse with geothermal heating system. *Acta Hortic* **2014**, *1037*, 113–118.
33. Ahamed, M.S.; Guo, H.; Tanino, K. Modeling heating demands in a chinese-style solar greenhouse using the transient building energy simulation model trnsys. *J. Build. Eng.* **2020**, *29*, 101114. [CrossRef]
34. Baglivo, C.; Mazzeo, D.; Panico, S.; Bonuso, S.; Matera, N.; Congedo, P.M.; Oliveti, G. Complete greenhouse dynamic simulation tool to assess the crop thermal well-being and energy needs. *Appl. Therm. Eng.* **2020**, *179*, 115698. [CrossRef]
35. Ritter, A.; Munoz-Carpena, R. Performance evaluation of hydrological models: Statistical significance for reducing subjectivity in goodness-of-fit assessments. *J. Hydrol.* **2013**, *480*, 33–45. [CrossRef]